International Journal of Bio-Inorganic Hybrid Nanomaterials

Calcination Treated of Mixed Spinel $ZnFe_2O_4$ Synthesized by Combustion Method

Esmat Nazari[1], Qazale Sadr Manuchehri[*2]

[1] *M.Sc., Department of Chemistry, Islamic Azad University, Tehran North Branch, Tehran, Iran*

[2] *M.Sc., Young Researchers and Elite Club, Pharmaceutical Sciences Branch, Islamic Azad University, Tehran, Iran*

ABSTRACT

$ZnFe_2O_4$ mixed spinel ferrite nanoparticles obtained through a citrate-nitrate combustion method. Ignited products calcined at different temperatures in 600-900ºC range and effect of calcination treatment temperature investigated. Final Products characterized by X-ray Diffraction (XRD), Fourier-Transform Infrared spectroscopy (FTIR), and Field Emission Scanning Electron Microscopy (FESEM). The average particle size calculated from Scherrer equation. Results demonstrate good agreement with total rule of increase in particle size by increasing of calcination temperature. Average particle size from X-ray data sheets for 900ºC was about 54 nm.

Keyword: Nano-powder; $ZnFe_2O_4$; Combustion; Surfactant; X-ray diffraction.

1. INTRODUCTION

Nanostructured materials are considered more than their bulk forms, due to quantum confinement that due to their advanced properties [1]. Cubic spinel ferrite nanoparticles such as Fe_3O_4, $MnFe_2O_4$, $NiFe_2O_4$ and $ZnFe_2O_4$ exhibit excellent magnetic properties, chemical stability and mechanical resistance [2, 3]. Among these, Zinc ferrite nanoparticles have wide applications such as T1 contrast agent [4], biomedicine applications [5], hyperthermia treatments [6], gas sensing [7-9], photo-catalysis [10], and photochemical water splitting [11]. This ferrite is of interest not only to technological applications as denoted, but also has great attrac-

tion to basic researches in their magnetic and electrical properties [1]. Based on cation distribution between A (tetrahedral) and B (octahedral) sites in spinel structure, these divided in two categories: normal spinel and reverse spinel. In normal spinel M^{2+} ions (M = Fe^{2+}, Mn^{2+}, Ni^{2+}, Zn^{2+}) occupied only tetrahedral sites and in reverse spinel where as it occupied only octahedral sites in an inverse one [12, 13]. Against bulk form, the nano-crystalline $ZnFe_2O_4$ system always shows up as a mixed spinel by distribution of Fe^{3+} and Zn^{2+} ions between A and B sites [14, 5]. Various synthesis methods developed to produce zinc ferrite nanoparticles, such

as simple and combine mechanical routes [15, 16], Precipitation [17-20], different type of Combustion reaction [1, 21-24]. Among these methods, combustion routes are highly interesting for their low cost and simplicity.

In this work, fine $ZnFe_2O_4$ nanoparticles have been synthesized via a simple combustion technique. Results demonstrate that calcination temperature play an important role in the phase formation and size controlling in this process.

2. MATERIALS AND METHODS

2.1. Materials
Zinc (II) nitrate tetra hydrate (98%), Iron (III) nitrate nona-hydrate (99-101%), Citric acid (99%) and Ammonia (25%) were purchased from Merck and Sigma-Aldrich Co. and used without any purification. Deionized water applied as solvent.

2.2. Synthesis of $ZnFe_2O_4$
Zinc ferrite nanoparticles were prepared successfully by means of a citrate-nitrate combustion method. Appropriate amount of metal nitrates in Zn:Fe, 1:2 molar ratio mixed together and solve in minimum amount of deionized water. Citric acid weighted in 1:3 ratios with metal nitrates, solves in minimum amount of deionized water, and added to metal nitrates solution. The pH of homogenized mixture adjusts at 7 by dropwise ammonia addition. After adequate heating

time (about 3 hours), viscous obtained gel expose at top of a burner flame. After some minutes gel was boiling and lose remain water. Next auto propagating combustion process start and gel transformed to loose powder. Obtained powders were calcined at 600, 700, 800, 900°C for 2 h, washed by ethanol and deionized water then solve in chloroform and irradiated in ultrasonic bath for 15 minutes characterized after drying and denoted as S1, S2, S3, S4, respectively.

2.3. Characterization process
Powder X-ray measurement was recorded with Philips, XPERT- MPD, operates at 40 kV and 30 mA. The morphology was investigated by using FESEM, Philips XL30 with 40 kV operating voltage. An FTIR spectrum was recorded as KBr pellets on Shimadzo, FTIR- 300 spectrophotometer.

3. RESULTS AND DISCUSSION

X-ray analysis presented at Figure 1. As shown in these four XRD patterns, four weak unmatched peak around 2theta 31, 33, 36, and 54 degrees attributed to presence of some impurity in samples S1, S2, and S3. As seems increase in calcination temperature due to decrease of these impurity peaks intensity. In S4 X-ray pattern, three peaks completely eliminated and the one remains in 32 degrees has very low intensity. The well matched peaks of S4 confirmed with JCPDS card No. 01-079-1150, for Zinc iron oxide by $ZnFe_2O_4$ stoi-
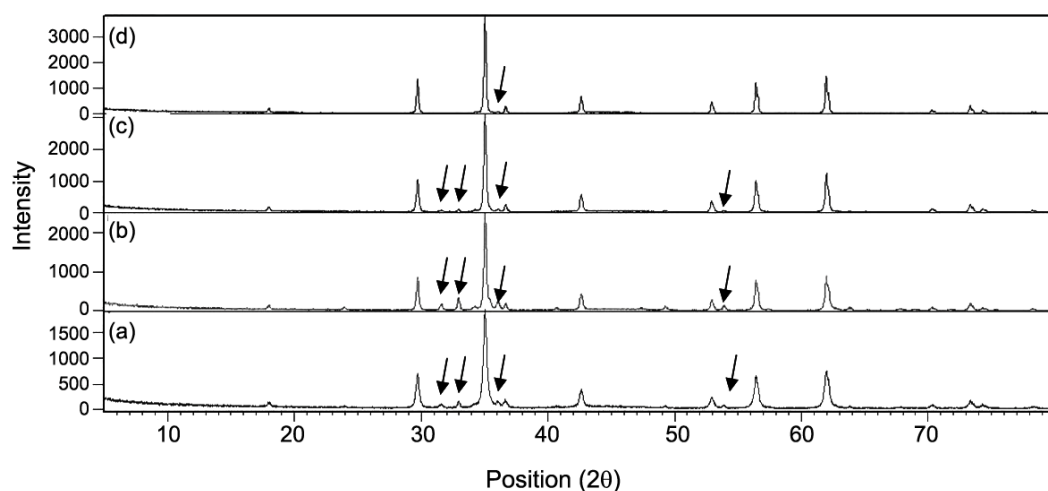

Figure 1: *X-ray diffraction pattern of (A) S1, (B) S2, (C) S3, (D) S4. (↙) means sub-phases (Fe_2O_3 and ZnO).*

Table 1: Chemical composition of calcined samples at different temperatures.

Sample name	Calcination temperature (ºC)	Phase composition	Average Crystallite size (nm)	Crystallinity percent (%)
S1	600	$ZnFe_2O_4$ Unmatched impurity	33	73.60
S2	700	$ZnFe_2O_4$ Unmatched impurity	40	73.33
S3	800	$ZnFe_2O_4$ Unmatched impurity	46	77.99
S4	900	$ZnFe_2O_4$	54	83.59

chiometric ferrite chemical formula.

The average crystallite sizes for main phase, $ZnFe_2O_4$ nano-particles, calculated using Scherrer's equation (Eq. 1).

$$d = K\lambda / \beta \cos\theta \qquad \text{(Eq. 1)}$$

Where d is the grain size, β is half-intensity width of the relevant diffraction; λ is X-ray wavelength and θ the diffraction angle.

The crystallinity percentage calculated from net to total area ratio obtained from X-ray data series. Sample compositions, Average crystallite size and Crystallinity percentage abstracted in Table 1.

The average crystallite size calculated from Scherrer's equation for fourth sample presented at Table 1. As calculated, the single phase S4 has 54 nm average crystallite size. Results demonstrate a slight increase in crystallite size by increase in calcination temperature. This was in good agreement by previous reports [25]. Obviously, when crystallite lattice can't abide applied treated temperatures may be broken up to subphase as occur in $MnFe_2O_4$ ferrites in temperatures up to 600°C or composed the new phases.

The FESEM images of S1 presented at Figure 2. As shown in these Figure $ZnFe_2O_4$ nanoparticles has a spherical shape. Against of ultrasound treatment before characterization, hard aggregations seem in some area, probably due to long period of calcination or presents of impurities.

The FTIR spectrum of selected sample, S1, illustrated at Figure 3. Characteristic vibrations around 3434 and 1628 cm^{-1} were indicated the asymmetric and symmetric H-O stretching bounds. The 675 and 547 cm^{-1} peak demonstrates metal-oxygen stretching

Figure 2: FESEM images of S1.
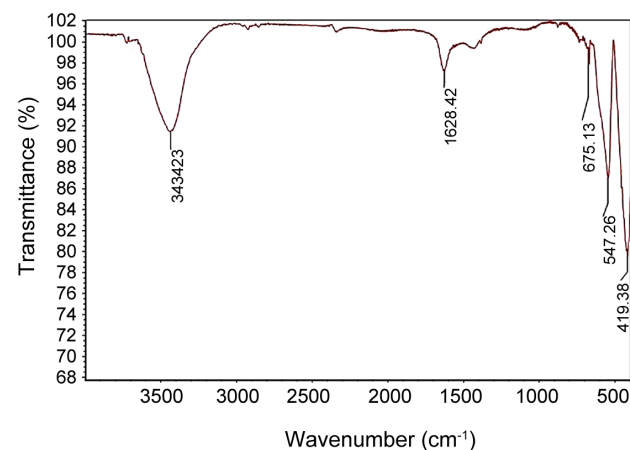
Figure 3: FTIR spectrum of S1.

bonds in tetrahedral situation. The intense peak in 419 cm^{-1} attributed to metal-oxygen stretching band in octahedral site. This result was in good agreement with some previous reports such as Wan et al. [4] and Prithviraj et al. [21].

4. CONCLUSIONS

Zinc ferrite nano-particles were produced successfully with the simple combustion method. Citrate-nitrate precursor selected and different calcination temperatures applied in burnt powders. Results demonstrate that particle size increase by increasing in calcination temperatures. Also, single phase composition obtained at 900ºC and in lower temperatures some impurities observed. For single phase sample, S4, particle size of 54 nm calculated.

REFERENCES

1. Manikhandan A., John Kennedy L., Bououndina M., Judith Vijaya J., *J. Magn. Magn. Mater.*, **349** (2014) 249.

2. Philip J., Gnanaprakash G., Panneerselvam G., Antony M.P., Jayakumar, Baldev Raj T., *J. Appl. Phys.*, **102** (2007) 1.

3. Zhao H., Zheng Zh., Wong K.W., Wang Sh., Huang B., Li D., *Electrochem. Commun.*, **9** (2007) 2606.

4. Wan J., Jiang X., Li H., Chen K., *J. Mater. Chem.*, **22** (2012) 13500.

5. Issa B., Obaidat Borhan I.M., Albiss A., Haik Y., *Int. J. Mol. Sci,.* **14** (2013) 21266.

6. Shah S.A., Hashmi M.U., Alam S., Shamim A., *J. Magn. Magn. Mater.*, **322** (2010) 375.

7. Xiangfeng Ch., Xingqin L., Guangyao M., *Sensors Actuat. B-Chem.*, **55** (1999) 19.

8. Chu X., Jiang D., Zheng Ch., *Mater. Sci. Eng. B*, **129** (2006) 150.

9. Y Patil J., Nadargi D.Y., Gurav J.L., Mulla I.S., Suryanshi Sh.S., *Ceram. Int.*, **40** (2014) 10607.

10. Habibi M.H., Habibi A.H., *J. Ind. Eng. Chem.*, **20** (2014) 2964.

11. Tahir A.A., Upul Wijayantha K.G., *J. Photoch. Photobio. A*, **216** (2010) 119.

12. Li F., Liu J., G.Evans D., Duan X., *Chem. Mater.*, **16** (2004) 11597.

13. Carta D., Casula M.F., Falqui A., Lonche D., Mountjoy G., Sangregorio C., Corrias A., *J. Phys. Chem. C*, **113** (2009) 8606.

14. Xu Y., Liang Y., Jiang L., Wu H., Zhao H., Xue D., *J. Nanomater.*, Volume 2011, Article ID 525967, 5 pages.

15. Yang H., Zhang X., Huang Ch., Yang W., Qiu G., *J. Phys. Chem. Solids*, **65** (2004) 1329.

16. Lazarevic Z.Z., Jovalekic C., Ivanovski V.N., Recnik A., Milutinovic A., Cekic B., Romecevic N.Z., *J. Phys. Chem. Solids*, **75** (2014) 869.

17. Ayyappan S., Paneerselvam G., Antony M.P., Philip J., *Mater. Chem. Phys.*, **128** (2011) 400.

18. Ladole Ch.A., *Int. J. Chem. Sci.*, **10** (2012) 1230.

19. Li J., Wang A., Lin Y., Liu X., Fu J., Lin L., *J. Magn. Magn. Mater.*, **330** (2013) 96.

20. Yelenich O.V., Solopan S.O., Kolodiazhnyi T.K., Dzyublyuk V.V., Tovstolytkin A.L., Brlous A.G., *Mater. Chem. Phys.*, **146** (2014) 129.

21. Prithviraj Swamy P.M., Basavaraja S., Lagashetty A., Srinivas Rao N.V., Nijagunappa R., Venkataraman A., *B. Mater. Sci.*, **34** (2011) 1325.

22. Sun S., Yang X., Zhang Y., Zhanf F., Ding J., Bao J., Gao Ch., *Prog. Nat. Sci.*, **22** (2012) 639.

23. Sutka S., Mezinskis G., Zamovskis M., Jakovkevs D., Pavlovska I., *Ceram. Int.*, **39** (2013) 8499.

24. Shanmugavani A., Kalai R., Layek S., Sanjeeraja C., *J. Magn. Magn. Mater.*, **354** (2014) 363.

25. Abedini Khorrami S., Mahmoudzadeha G., Madani S.S., Gharib F., *J. Ceram. Process. Res.*, **12** (2011) 504.